Inorg. Chem. **2008**, *47*, 2267−2273

Phenomenally High Molar Extinction Coefficient Sensitizer with "Donor−Acceptor" Ligands for Dye-Sensitized Solar Cell Applications

Chongchan Lee,[‡] Jun-Ho Yum,[†] Hyunbong Choi,[‡] Sang Ook Kang,[‡] Jaejung Ko,*[,‡] Robin Humphry-Baker,[†] Michael Grätzel,[†] and Md. K. Nazeeruddin*[,†]

Laboratory for Photonics and Interfaces, Station 6, Institute of Chemical Sciences and Engineering, School of Basic Sciences, Swiss Federal Institute of Technology, CH-1015 Lausanne, Switzerland, and Department of Chemistry, Korea University, Jochiwon, Chungnam 339-700, Korea

Received May 22, 2007

A phenomenally high molar extinction coefficient heteroleptic ruthenium(II) complex [Ru(4,4′-carboxylic acid-2,2′-bipyridine)(4,4′-(4-{4-methyl-2,5-bis[3-methylbutoxy]styryl}-2,5-bis[3-methylbutoxy]-2,2′-bipyridine)(NCS)$_2$] (**DCSC13**) was synthesized by incorporating donor−acceptor ligands. The absorption spectrum of the **DCSC13** sensitizer is dominated by metal-to-ligand charge-transfer transitions (MLCT) in the visible region, with absorption maxima appearing at 442 and 554 nm. The lowest MLCT absorption bands are red-shifted, and the molar extinction coefficients of these bands are significantly higher at 72 100 and 30 600 M^{-1} cm^{-1}, respectively, when compared to those of the analogous [Ru(4,4′-carboxylic acid-2,2′-bipyridine)(4,4′-dimethyl-2,2′-bipyridine)(NCS)$_2$] (**N820**) sensitizer. The **DCSC13** complex, when anchored on nanocrystalline TiO_2 films, exhibited increased short-circuit photocurrent and consequent power-conversion efficiency when compared with the **N820** sensitizer.

Introduction

Dye-sensitized solar cells (DSSC) based on mesoporous nanocrystalline TiO_2 films have attracted significant attention as low-cost devices and can reach sunlight-to-electric power-conversion efficiencies of 8–11%.[1] In these cells, the sensitizer is one of the key components for high power-conversion efficiency, and the *cis*-dithiocyanato-bis(2,2′-bipyridyl-4,4′-dicarboxylic acid)Ru(II) complex (**N3**) is the most-efficient heterogeneous charge-transfer sensitizer that is widely used in the nanocrystalline TiO_2-based dye-sensitized solar cell.[2–12] Efficient charge transfer occurs after anchoring of the sensitizer through a carboxylate group onto the surface of the TiO_2 semiconductor.[13] The immobilized sensitizer forms a monomolecular film on the TiO_2 surface, thereby facilitating charge transfer by electron injection. However, the main drawback of the **N3** sensitizer is the lack of absorption in the red region of the visible spectrum and also the relatively low molar extinction coefficient.[14] The sensitizers with an enhanced molar extinction coefficient allow a reduction in film thickness and thus are more efficient because of reduced transport losses in the nanoporous environment, leading to increased open-circuit potentials.[15]

In quest of such sensitizers, we have designed and developed a high molar extinction coefficient sensitizer

* To whom correspondence should be addressed. E-mail: mdkhaja.nazeeruddin@epfl.ch.
‡ Korea University.
† Swiss Federal Institute of Technology.

(1) Nazeeruddin, M. K.; De Angelis, F.; Fantacci, S.; Selloni, A.; Viscardi, G.; Liska, P.; Ito, S.; Bessho, T.; Grätzel, M. *J. Am. Chem. Soc.* **2005**, *127*, 16835–16847.
(2) Grätzel, M. *Nature* **2001**, *414*, 338.
(3) Asbury, J. B.; Ellingson, R. J.; Gosh, H. N.; Ferrere, S.; Notzig, A. J.; Lian, T. *J. Phys. Chem. B* **1999**, *103*, 3110–3119.
(4) Park, N.-G.; Kang, M. G.; Kim, K. M.; Ryu, K. S.; Chang, S. H.; Kim, D.-K.; Van de Lagemaat, J.; Benkstein, K. D.; Frank, A. J. *Langmuir* **2004**, *20*, 4246–4253.
(5) Heimer, T. A.; Heilweil, E. J.; Bignozzi, C. A.; Meyer, G. J. *J. Phys. Chem. A* **2000**, *104*, 4256–4262.
(6) Saito, Y.; Fukuri, N.; Senadeera, R.; Kitamura, T.; Wada, Y.; Yanagida, S. *Electrochem. Commun.* **2004**, *6*, 71–74.
(7) Bisquert, J.; Cahen, D.; Hodes, G.; Ruehle, S.; Zaban, A. *J. Phys. Chem. B* **2004**, *108*, 8106–8118.
(8) Fabregat-Santiago, F.; Garcia-Canadas, J.; Palomares, E.; Clifford, J. N.; Haque, S. A.; Durrant, J. R.; Garcia-Belmonte, G.; Bisquert, J. *J. Appl. Phys.* **2004**, *96*, 6903–6907.
(9) Figgemeier, E.; Hagfeldt, A. *Int. J. Photoenergy* **2004**, *6*, 127–140.
(10) Furube, A.; Katoh, R.; Yoshihara, T.; Hara, K.; Murata, S.; Arakawa, H.; Tachiya, M. *J. Phys. Chem. B* **2004**, *108*, 12588–12592.
(11) Lee, J.-J.; Coia, G. M.; Lewis, N. S. *J. Phys. Chem. B* **2004**, *108*, 5269–5281.
(12) Miyasaka, T.; Kijitori, Y. *J. Electrochem. Soc.* **2004**, *151*, A1767–A1773.
(13) Fillinger, A.; Parkinson, B. A. *J. Electrochem. Soc.* **1999**, *146*, 4559.

10.1021/ic700996x CCC: $40.75
Published on Web 09/07/2007

Scheme 1. Synthesis of 4,4′-(Di(2,5-dimethylbutoxyphenyl)ethenyl)-2,2′-bipyridine

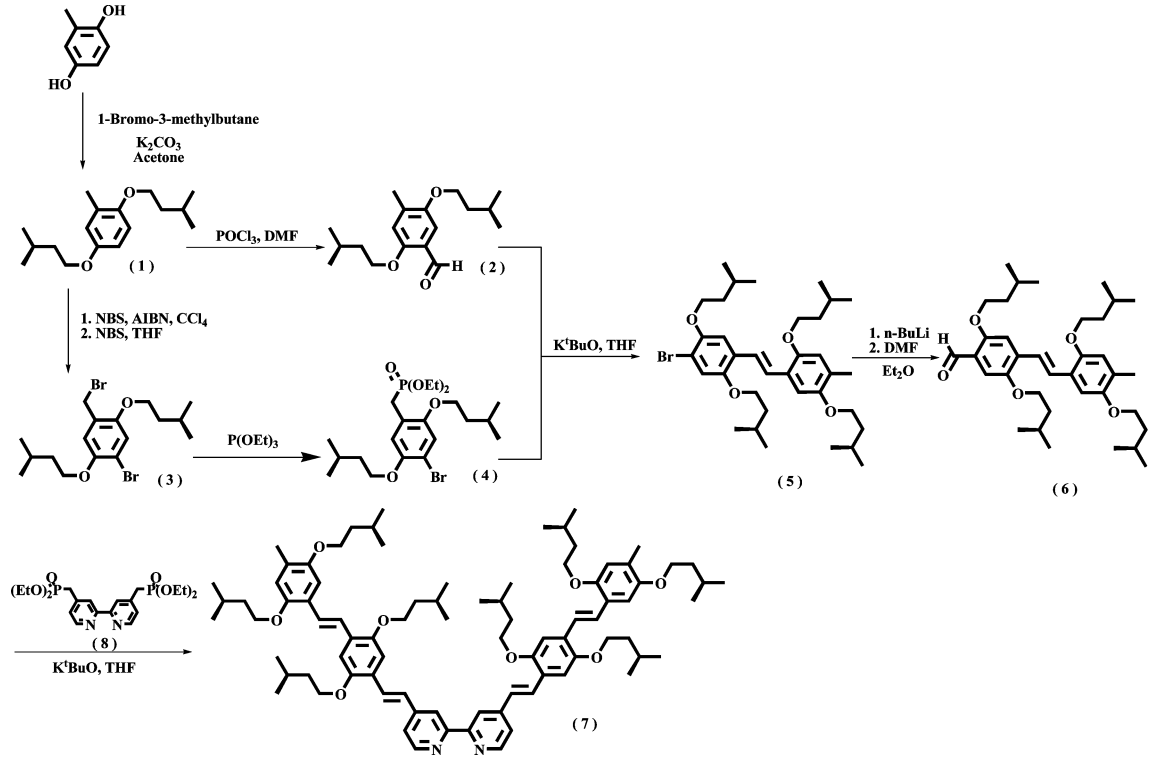

[Ru(4,4′-dicarboxylic acid-2,2′-bipyridine)(4,4′-(4-{4-methyl-2,5-bis[3-methylbutoxy]styryl}-2,5-bis[3-methylbutoxy]-2,2′-bipyridine)$(NCS)_2$] (**DCSC13**). In **DCSC13**, the 4,4′-dicarboxylic acid-2,2′-bipyridine acts as the anchoring group, and the 4,4′-(4-{4-methyl-2,5-bis[3-methylbutoxy]styryl}-2,5-bis[3-methylbutoxy]-2,2′-bipyridine acts as the donor ligand, which enhances the molar extinction coefficient significantly when compared to that of the analogous [Ru(4,4′-carboxylic acid-2,2′-bipyridine)(4,4′-dimethyl-2,2′-bipyridine)$(NCS)_2$] sensitizer. The insertion of 4,4′-(4-{4-methyl-2,5-bis[3-methylbutoxy]styryl}-2,5-bis-3-methylbutoxy groups on the 2,2′-bipyridine enhances the molar extinction coefficient, and the substituted methoxy groups tune the LUMO level of the ligand to provide directionality in the excited state.[15] The function of the thiocyanato ligands is to tune the metal t_{2g} orbitals of ruthenium(II) and possibly to stabilize the hole that is being generated on the metal, after having injected an electron into the conduction band. In this article, we report the synthesis, characterization, and photovoltaic properties of high molar extinction coefficient ruthenium(II) complex **DCSC13**.

Experimental Section

All of the reactions were carried out under an argon atmosphere. THF and ether were distilled from sodium. ^1H, ^{13}C, and ^{31}P NMR spectra were recorded on a Varian Mercury 300 spectrometer. UV−vis spectra were recorded in a 1 cm path length quartz cell on a Cary 5 spectrophotometer. Emission spectra were recorded on a Spex Fluorolog 112 using a 90° optical geometry. The emitted light was detected with a Hamamatsu R928 photomultiplier operated in single-photon counting mode. The emission spectra were photometrically corrected using an NBS-calibrated 200 W tungsten lamp as a reference source. The photoelectrochemical measurements were carried out using a xenon lamp source designed to give 100 mW/cm^2 at AM 1.5G sunlight and a voltage source meter to sweep a voltage across the irradiated cell and at the same time measure as the generated current. The IPCE is determined by wavelength scanning the light source on the cell and measuring the short-circuit current as a function of wavelength.[23] Photogenerated transients were observed using an exciting pulse generated by red light emitting diodes with a white-light bias. From the current decay, the photogenerated charge in the cell is measured. The corresponding voltage decay gives the electron lifetime. Electrochemical data were obtained by cyclic voltammetry using a three-electrode cell and an Auto laboratory System (PGSTAT 30, GPES 4.8 software). The working electrode was a 0.03 cm^2 glassy-carbon disk, the auxiliary electrode was a glassy-carbon rod, and a silver disk of 0.03 cm^2 was used as the quasi-reference electrode. The sensitizers were dissolved in dimethylformamide (DMF) containing 0.1 M tetrabutylammonium hexafluorophosphate as the supporting electrolyte. After the measurement, ferrocene was added as the internal reference for calibration. All of the starting materials were purchased from either Aldrich or Strem and used without further purification. Scheme 1 shows the synthetic strategy used to afford the ligand 4,4′-(4-{4-methyl-2,5-bis[3-methylbutoxy]styryl}-2,5-bis[3-methylbutoxy]-2,2′-bipyridine.

1,4-Bis[3-methylbutoxy]-2-methylbenzene (1). 1-Bromo-3-methylbutane (26.77 g, 177 mmol) was added to a suspension of methylhydroquinone (10.0 g, 81 mmol) and K_2CO_3 (55.67 g, 403 mmol) in dry acetone (250 mL) under an atmosphere of dry argon.

(14) Nazeeruddin, M. K.; Kay, A.; Rodicio, I.; Humphry-Baker, R.; Muller, E.; Liska, P.; Vlachopoulos, N.; Grätzel, M. *J. Am. Chem. Soc.* **1993**, *115*, 6382.

(15) Nazeeruddin, M. K.; Wang, Q.; Cevey, L.; Aranyos, V.; Liska, P.; Figgemeier, E.; Klein, C.; Hirata, N.; Koops, S.; Haque, S. A.; Durrant, J. R.; Hagfeldt, A.; Lever, A. B. P.; Grätzel, M. *Inorg. Chem.* **2006**, *45*, 787–797.

The reaction mixture was stirred for 24 h at reflux temperature. After the mixture was cooled to room temperature, the solvent was removed in a vacuum. The resulting crude product was purified by column chromatography (silica gel, CH_2Cl_2/hexane 1:4, $R_f = 0.5$). Evaporation of the solvent yielded 18.2 g (85%) of **1** as a colorless oil. ^{1}H NMR ($CDCl_3$): δ 6.77 (d, 1H), 6.75 (s, 1H), 6.70 (d, 1H), 3.95 (m, 4H), 2.23 (s, 3H), 1.86 (m, 2H), 1.69 (m, 4H), 0.99 (m, 12H); $^{13}C^{16}$ NMR ($CDCl_3$): δ 152.9, 151.6, 128.2, 117.8, 112.2, 111.7, 67.2, 67.0, 38.4, 38.3, 25.3, 25.2, 22.8, 22.7, 16.5. Anal. Calcd for $C_{17}H_{28}O_2$: C, 77.22; H, 10.67. Found: C, 77.05; H, 10.58.

2,5-Bis[3-methylbutoxy]-4-methylbenzaldehyde (2). $POCl_3$ (13.92 g, 90.77 mmol) was added to a mixture of **1** (6 g, 22.69 mmol) and DMF (6.6 g, 90.77 mmol) under an atmosphere of dry argon. The reaction mixture was stirred for 12 h at reflux temperature. After the mixture was cooled to room temperature, the mixture was poured on ice–water (100 mL), stirred for 1 h, and extracted with diethyl ether (200 mL); during the extraction, NaCl was added to promote phase separation. The organic phase was washed with 1 M HCl (3 × 100 mL), water (3 × 100 mL), and a saturated $NaHCO_3$ solution (100 mL). After the organic phase was dried over $MgSO_4$ and the solvent was evaporated in a vacuum, the crude product was purified by column chromatography (silica gel, CH_2Cl_2/hexane 1:2, $R_f = 0.4$). Recrystallization from methanol yielded 5.3 g (80%) of **2** as white crystals. ^{1}H NMR ($CDCl_3$): δ 10.40 (s, 1H), 7.22 (s, 1H), 6.79 (s, 1H), 4.04 (t, 2H), 3.97 (t, 2H), 2.26 (s, 3H), 1.83 (m, 2H), 1.69 (m, 4H), 0.96 (m, 12H); $^{13}C^{16}$ NMR ($CDCl_3$): δ 189.5, 156.3, 151.5, 136.9, 123.1, 115.7, 108.3, 67.6, 66.9, 38.1, 38.0, 25.3, 25.2, 22.8, 22.7, 17.4. Anal. Calcd for $C_{18}H_{28}O_3$: C, 73.93; H, 9.65. Found: C, 73.74; H, 9.57.

1-Bromo-2,5-bis[3-methylbutoxy]-4-bromomethylbenzene (3). NBS (4.0 g, 22.7 mmol) and AIBN (1.1 g, 6.8 mmol) were added to a solution of **1** (5.0 g, 18.9 mmol) in dry CCl_4 (30 mL) under an atmosphere of dry argon. After the reaction mixture was stirred for 1 h under reflux, it was subsequently allowed to cool to room temperature and was filtered. After evaporation of the solvent, hexane (60 mL) was added to the residue, and the resulting suspension was filtered and evaporated to dryness. The remaining residue was dissolved in dry THF (30 mL); NBS (4.4 g, 24.6 mmol) was added, and the reaction mixture was stirred at reflux temperature for 1 h. After evaporation of the solvent, hexane (60 mL) was added. The solution was filtered, and the solvent was removed in a vacuum. Crystallization of the residue from ethanol yielded 3.6 g (45%) of **3** as a white crystalline solid. ^{1}H NMR ($CDCl_3$): δ 7.06 (s, 1H), 6.90 (s, 1H), 4.50 (s, 2H), 3.99 (t, 4H), 1.89 (m, 2H), 1.71 (m, 4H), 0.99 (m, 6H), 0.96 (t, 6H); $^{13}C^{16}$ NMR ($CDCl_3$): δ 151.7, 150.0, 126.6, 117.9, 116.5, 113.7, 69.1, 68.1, 38.7, 38.5, 29.0, 25.7, 25.6, 23.2, 23.1. Anal. Calcd for $C_{17}H_{26}Br_2O_2$: C, 48.36; H, 6.21. Found: C, 48.11; H, 6.11.

Diethyl{2,5-bis[3-methylbutoxy]-4-bromobenzyl}phosphonate (4). Triethyl phosphite (10 mL) and **3** (3.2 g, 7.6 mol) were stirred at 160 °C for 1.5 h while the liberated ethyl bromide was distilled off. The reaction mixture was cooled to 75 °C, and the excess triethyl phosphite was removed by distillation under reduced pressure to leave **4** (3.6 g, 100%) as a white solid. ^{1}H NMR ($CDCl_3$): δ 7.03 (s, 1H), 6.96 (d, $J_{H-P} = 2.7$ Hz, 1H), 4.02 (q, 4H), 3.92 (t, 4H), 3.17 (d, 2H, $J_{H-P} = 21.9$ Hz), 1.84 (m, 2H), 1.67 (m, 4H), 1.24 (t, 6H), 0.96 (d, 6H), 0.94 (d, 6H); $^{13}C^{16}$ NMR ($CDCl_3$): δ 151.9, 149.3, 127.1, 117.0, 116.4, 109.0, 76.2, 68.9, 67.4, 38.3, 38.2, 25.3, 25.2, 22.8, 22.7, 22.2, 16.4; ^{31}P NMR ($CDCl_3$): δ 20.95. Anal. Calcd for $C_{21}H_{36}BrO_5P$: C, 52.61; H, 7.57. Found: C, 52.46; H, 7.48.

4-{4-Methyl-2,5-bis[3-methylbutoxy]styryl}-2,5-bis[3-methylbutoxy]bromobenzene (5). A solution of aldehyde **2** (1.52 g, 5.2 mmol) in dry THF (20 mL) was added dropwise to a solution of **4** (2.50 g, 5.2 mmol) and *t*-BuOK (0.70 g, 6.2 mmol) in dry THF (30 mL) under an atmosphere of dry argon. The reaction mixture was stirred for 8 h at room temperature and subsequently poured onto crushed ice (60 g). Aqueous HCl (5 M, 20 mL) was added, and the aqueous phase was extracted with $CHCl_3$ (3 × 30 mL). The combined organic layers were washed with 3 M HCl and dried over $MgSO_4$. The solvent was evaporated. **5** (1.93 g, 60%) was obtained as a yellow solid after recrystallization from ethanol. ^{1}H NMR ($CDCl_3$): δ 7.44 (d, 1H), 7.32 (d, 1H), 7.16 (s, 1H), 7.07 (s, 1H), 7.06 (s, 1H), 6.73 (s, 1H), 4.00 (m, 8H), 2.23 (s, 3H), 1.89 (m, 4H), 1.73 (m, 8H), 0.99 (m, 12H), 0.97 (m, 12H); $^{13}C^{16}$ NMR ($CDCl_3$): δ 151.6, 150.9, 150.5, 149.9, 127.9, 127.5, 124.8, 124.2, 121.7, 117.8, 116.0, 111.6, 111.2, 109.0, 68.6, 68.3, 68.0, 67.1, 38.5, 38.4, 38.2, 38.1, 25.5, 25.4, 25.3, 25.1, 22.9, 22.8, 22.7, 22.6, 16.6. Anal. Calcd for $C_{35}H_{53}BrO_4$: C, 68.06; H, 8.65. Found: C, 68.04; H, 8.58.

4-{4-Methyl-2,5-bis[3-methylbutoxy]styryl}-2,5-bis[3-methylbutoxy]benzaldehyde (6). Bromide **5** (1.7 g, 2.75 mmol) was dissolved in dry diethyl ether (30 mL). The solution was cooled to −10 °C, and 1.6 M *n*-butyllithium in hexane (2.1 mL, 3.3 mmol) was added slowly. After the mixture was stirred for 30 min, the cooling bath was removed, and dry DMF (0.97 mL, 12.56 mmol) was added dropwise. The mixture was stirred for another hour at room temperature. After the addition of 6 M HCl (20 mL), the organic layer was washed with water (100 mL), with a saturated $NaHCO_3$ solution (50 mL), and again with water (30 mL). The organic layer was dried over $MgSO_4$, and the solvent was evaporated in a vacuum. The crude product was purified by column chromatography (silica gel, CH_2Cl_2/hexane 1:1, $R_f = 0.4$). Recrystallization from methanol yielded 1.1 g (80%) of **6** as a yellow solid. ^{1}H NMR ($CDCl_3$): δ 10.43 (s, 1H), 7.60 (d, 1H), 7.44 (d, 1H), 7.32 (s, 1H), 7.22 (s, 1H), 7.08 (s, 1H), 6.74 (s, 1H), 4.04 (m, 8H), 2.24 (s, 3H), 1.88 (m, 4H), 1.75 (m, 8H), 1.00 (m, 12H), 0.98 (m, 12H); $^{13}C^{16}$ NMR ($CDCl_3$): δ 189.3, 156.4, 151.7, 150.9, 150.6, 135.5, 128.9, 127.3, 124.3, 123.9, 121.5, 116.0, 110.1, 110.0, 109.2, 68.0, 67.6, 67.4, 67.2, 38.4, 38.3, 38.2, 38.1, 25.5, 25.4, 25.3, 25.2, 22.9, 22.8, 22.7, 22.6, 16.7. Anal. Calcd for $C_{36}H_{54}O_5$: C, 76.28; H, 9.60. Found: C, 76.02; H, 9.59.

4,4′-(4-{4-Methyl-2,5-bis[3-methylbutoxy]styryl}-2,5-bis[3-methylbutoxy]-2,2′-bipyridine (7). A solution of aldehyde **6** (0.66 g, 1.2 mmol) in dry THF (20 mL) was added dropwise to a solution of **8** (0.24 g, 0.5 mmol) and *t*-BuOK (0.14 g, 1.2 mmol) in dry THF (30 mL) under an atmosphere of dry argon.[17] The reaction mixture was stirred for 8 h at room temperature. The solvent was evaporated in a vacuum. Aqueous HCl (5 M, 20 mL) was added, and the aqueous phase was extracted with CH_2Cl_2 (3 × 30 mL). The combined organic layers were washed with 3 M HCl and dried over $MgSO_4$. The solvent was evaporated in a vacuum. The crude product was purified by column chromatography (silica gel, ethyl acetate/hexane 1:3, $R_f = 0.4$) and **7** (0.38 g, 25%) was obtained as a yellow solid. ^{1}H NMR ($CDCl_3$): δ 8.67 (s, 2H, $J = 5.1$ Hz, *pyridine*), 8.52 (s, 2H, *pyridine*), 7.79 (d, 2H, $J = 16.5$ Hz, *vinyl-H*), 7.51 (d, 2H, $J = 16.2$ Hz, *vinyl-H*), 7.44 (d, 2H, $J = 5.7$ Hz, *pyridine*), 7.43 (d, 2H, $J = 16.2$ Hz, *vinyl-H*), 7.21 (d, 2H, $J =$

(16) K8, c.; Anal. $C_{34}H_{24}N_6O_8RuS_2$: cf. C; H; N. Found: C; H; N; ^{1}H NMR (dH/ppm in DMSO-d_6, J. H. d., H 6,5, J 5.9); 9.27 (d, H, 5); 9.15 (s, H, 3); 8.99. (s, H; 8.21 (dd, H, 6,3, J 5.9; 1); 7.8 (d, v.-H., J 15.94); 7.62 (d, H, 5′, J 5.9); 7.55 (d, v.-H., J 15.97); 7.45 (dd, H, 6′3′, J 5.9; 1); 7.21 (d, v.-H., J 16.04); 6.99 (d, v.-H., J 16.04).

(17) Gould, S.; Meyer, T. J.; Strouse, G. F.; Sullivan, B. P. *Inorg. Chem.* **1991**, *30*, 2942.

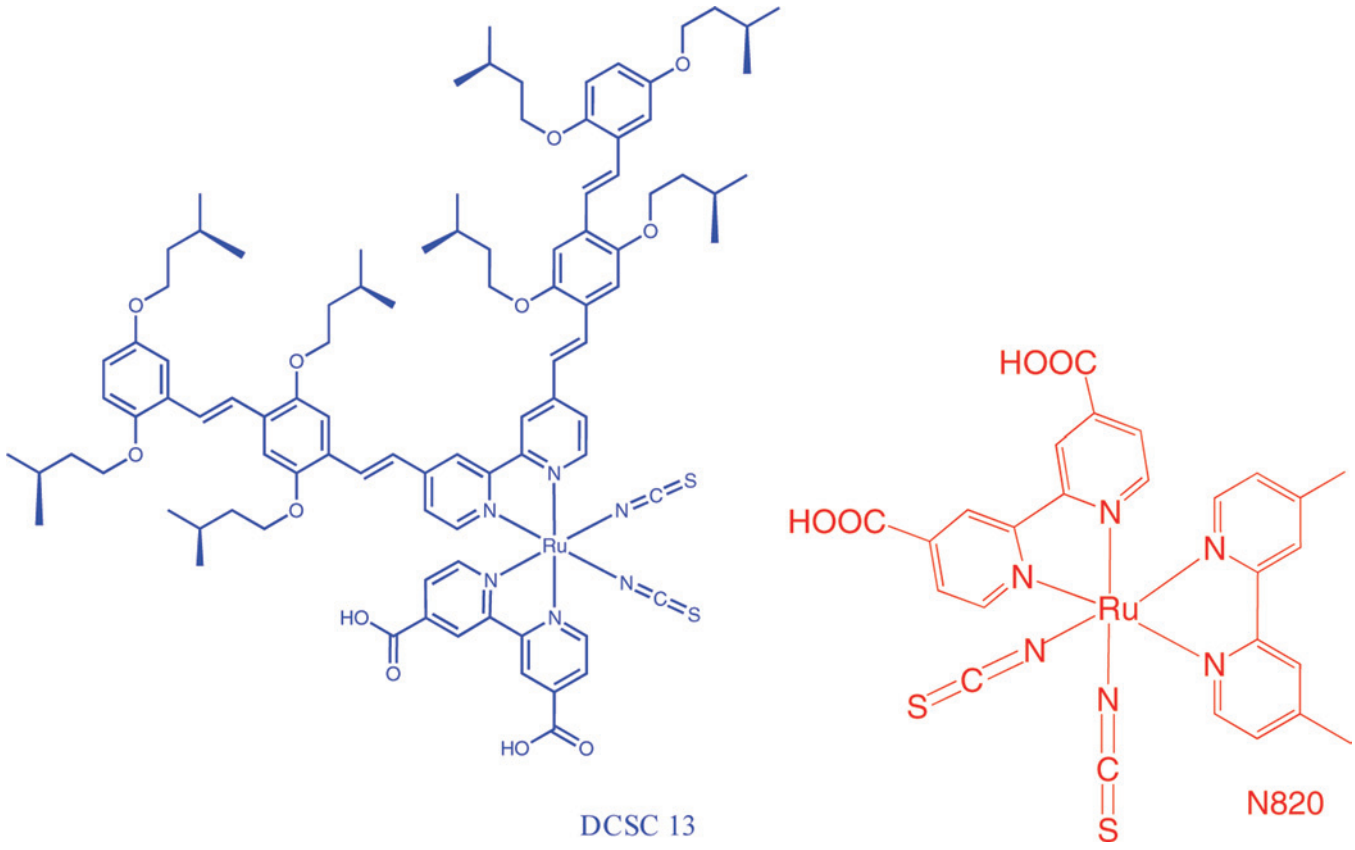

Figure 1. Chemical structures of **DCSC13** and **N820** sensitizers.

16.5 Hz, *vinyl-H*), 7.20 (s, 2H), 7.15 (s, 2H), 7.10 (s, 2H), 6.74 (s, 2H), 4.10 (m, 8H), 4.06 (m, 8H), 2.24 (s, 6H), 1.92 (m, 8H), 1.79 (m, 16H), 1.01 (m, 48H); $^{13}C^{16}$ NMR ($CDCl_3$): δ 156.7, 151.7, 151.6, 150.8, 150.6, 149.5, 146.6, 129.1, 128.4, 128.0, 126.2, 125.1, 125.0, 124.3, 121.9, 120.5, 119.0, 116.1, 111.1, 110.0, 109.0, 68.1, 68.0, 67.8, 67.2, 38.5, 38.4, 38.3, 38.2, 25.6, 25.5, 25.4, 25.3, 22.9, 22.8, 16.6. Anal. Calcd for $C_{36}H_{54}O_5$: C, 78.71; H, 9.12. Found: C, 78.58 H, 9.05.

[Ru(II)LL′(NCS)$_2$] (L = 4,4′-(4-{4-Methyl-2,5-bis[3-methylbutoxy]styryl}-2,5-bis[3-methylbutoxy]-2,2′-bipyridine, L′ = 4,4′-(Dicarboxylic acid)-2,2′-bipyridine), DCSC13. 4,4′-(4-{4-Methyl-2,5-bis[3-methylbutoxy]styryl}-2,5-bis[3-methylbutoxy]-2,2′-bipyridine ligand (0.22 g, 0.17 mmol) and dichloro(*p*-cymene)ruthenium(II) dimer (0.051 g, 0.084 mmol) in DMF were heated at 80 °C for 4 h under argon in the dark. After this period, 4,4′-dicarboxylic acid-2,2′-bipyridine (41 mg, 0.17 mmol) was added, and the reaction mixture was heated to 160 °C for another 4 h. To the resulting dark-green solution was added solid NH_4NCS (0.19, 2.7 mmol), and then the reaction mixture was further heated for 4 h at 130 °C. DMF was removed on a rotary evaporator under a vacuum, and water (20 mL) was added to get the precipitate. The purple solid was filtered off, washed with water and Et_2O, and dried under a vacuum. The crude compound was dissolved in basic methanol (with TBAOH) and further purified three times on the Sephadex LH-20 with methanol as the eluent. The main band was collected, concentrated, and precipitated with acidic methanol (HNO_3) to obtain pure **DCSC13**. ^{1}H NMR (DMSO): δ 9.38 (d, 1H), 9.17 (d, 1H,), 9.05 (s, 1H), 8.90 (s, 1H), 8.86 (s, 1H), 8.71 (s, 1H), 8.26 (d, 1H), 8.05 (d, 1H), 7.8∼6.8 (m, 20H), 4.04 (m, 16H), 2.17 (s, 3H), 2.15 (s, 3H), 1.84 (m, 8H), 1.67 (m, 16H), 0.96 (m, 48H). Anal. Calcd for $C_{98}H_{124}N_6O_{12}RuS_2$: C, 67.52; H, 7.17; N, 4.82. Found: C, 67.38; H, 7.10; N, 4.75.

Results and Discussion

4,4′-(4-{4-Methyl-2,5-bis[3-methylbutoxy]styryl}-2,5-bis[3-methylbutoxy]-2,2′-bipyridine (**7**) was synthesized in seven steps using *o*-alkylation, bromination, the Vilsmeier−Haack reaction, the phosphonate reaction, and the Wittig coupling reaction, as shown in Scheme 1. **DCSC13** was obtained in one pot synthesis from the sequential reaction of the [Ru(*p*-cymene)Cl_2]$_2$ dimer with **7** and the reaction of the resulting mononuclear complex with 4,4′-dicarboxyl-2,2′-bipyridine, followed by the addition of an excess of ammonium thiocyanate ligand. The crude complex was purified three times on a Sephadex LH-20 column to remove impurities and sulfur-bonded isomers using methanol as an eluent. The analytical and the spectroscopic data of **DCSC13** are fully consistent with the formulated structure.

The absorption spectrum of the **DCSC13** sensitizer, shown in Figure 2, is dominated in the visible region by absorption features at 442 and 554 nm, and in the UV region at 310 and 334 nm. The bands in the visible region are assigned to metal-to-ligand charge-transfer transitions (MLCT) and in the UV regions to ligand π–π^* transitions.[18] The lowest-energy MLCT band in the **DCSC13** complex is red-shifted by 34 nm when compared to the [Ru(4,4′-carboxylic acid-2,2′-bipyridine)(4,4′-dimethyl-2,2′-bipyridine)(NCS)$_2$] (**N820**) sensitizer, and the molar extinction coefficients of the visible absorption bands at 442 and 554 nm are 72 100 and 30 600 M^{-1} cm^{-1}, respectively, which

(18) Ryan, M. F.; Metcalfe, R. A.; Lever, A. B. P.; Haga, M.-A. *J. Chem. Soc., Dalton Trans.* **2000**, 2357.

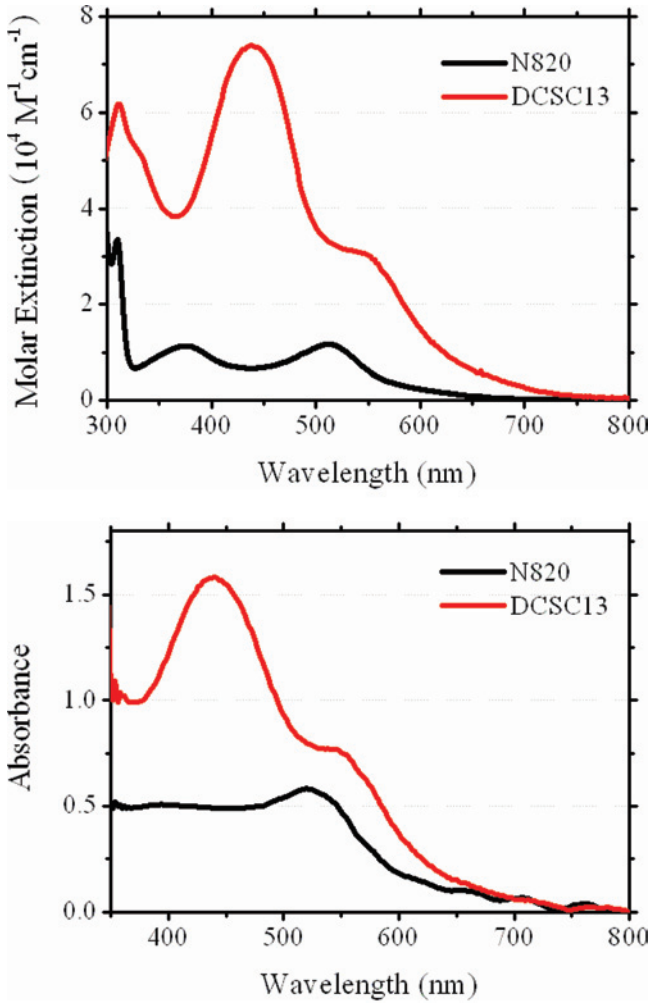

Figure 2. A comparison of UV−vis absorption spectra of **DCSC13** (red, 3×10^{-5}) and **N820** (black, 3.5×10^{-5}) complexes in ethanol (top panel), and adsorbed on a nanocrystalline 2 µm thick transparent TiO_2 film (bottom panel), a similar 2 µm thick TiO_2 nanocrystalline film was used as a reference.

are significantly higher than those of the analogous **N820** sensitizer, which possess only 11 600 M^{-1} cm^{-1}. The red shift is due to destabilization of the HOMO orbitals' resulting MLCT transitions that occur at lower energies.[19] The absorption spectra of both of the sensitizers adsorbed on a 2 µm transparent TiO_2 film show features similar to those seen in the corresponding solution spectra but exhibit a slight red-shift of 5 nm due to the interaction of the anchoring groups to the surface (Figure 2). The solution absorption spectra reveal that the molar extinction coefficient of **DCSC13** is 2.6 times higher than the [Ru(4,4′-carboxylic acid-2,2′-bipyridine)(4,4′-dimethyl-2,2′-bipyridine)$(NCS)_2$] (**N820**) sensitizer for the lowest-energy transition.[20] However, the optical density of **DCSC13** adsorbed onto 2 µm transparent TiO_2 film shows only a 1.2 times increase to that of the **N820** sensitizer. The adsorbed sensitizers were desorbed using an alkaline ethanol solution, which show that the amount of adsorbed **DCSC13** molecules onto the TiO_2 surface was only $\sim 5 \times 10^{-8}$ mol/cm^2, 40% when compared to **N820** sensitizer, $\sim 1.4 \times 10^{-7}$ mol/cm^2. The low adsorption of the **DCSC13** sensitizer onto a 2 µm transparent TiO_2 film is due to its larger size compared to that of the **N820** sensitizer, preventing penetration into the nanoporous film.

Emission data of the **DCSC13** complex were obtained by exciting within the MLCT absorption band at 298 K in an air-equilibrated ethanol solution. **DCSC13** exhibits a luminescence maximum at 850 nm, which is 100 nm red-shifted compared to that of the **N820** emission and consistent with the shift in the lowest-MLCT absorption band. The cyclic voltammogram of **DCSC13** obtained using a glassy-carbon disk electrode in a dimethylformamide solvent with 0.1 M tetrabutylammonium hexafluorophosphate as the supporting electrolyte exhibits a quasi-reversible oxidation at $E_{1/2} = 0.21$ V versus ferrocene (Fc). When scanning toward negative potentials, one quasi-reversible wave at $E_{1/2} = -1.8$ V is observed, which is assigned to the 4,4′-dicarboxylic acid-2,2′-bipyridine-based reduction.

TiO_2 nanoparticles (avg = 20 nm) were synthesized by hydrothermal crystallization in basic solution with NH_4OH, converted to the TiO_2 screen-printing paste, resulting in semiopaque TiO_2 film.[21] The screen-printed thin 2 µm transparent film was prepared and treated with a 40 mM titanium tetrachloride solution, using a previously reported procedure.[1,22] The film was sintered at 500 °C in air for 30 min before use. The TiO_2 electrodes were immersed into the **DCSC13** and **N820** solutions (0.3 mM in a mixture of acetonitrile and *tert*-butyl alcohol, volume ratio of 1:1) and kept at room temperature for 18 h. The dye-adsorbed TiO_2 electrode and the platinum counter electrode were assembled into a sealed sandwich-type cell by heating with a hot-melt ionomer film (Surlyn 1702, 25 µm thickness, Du Pont) as a spacer between the electrodes. The fabrication procedure for solar cells, the testing conditions, and the equipment used were reported before.[1]

The incident monochromatic photon-to-current conversion efficiency (IPCE) is defined as the number of electrons generated by light in the external circuit divided by the number of incident photons as a function of excitation wavelength. Figure 3 shows the IPCE obtained with a sandwich cell using a 2 µm transparent photoanode containing an electrolyte of 0.6 M *M*-methyl-*N*-butyl imidiazolium iodide, 0.04 M iodine, 0.025 M LiI, 0.05 M guanidinium thiocyanate, and 0.28 M *tert*-butylpyridine in a 15:85 (v/v) mixture of valeronitrile and acetonitrile. The IPCE of **DCSC13** and **N820** plotted as a function of excitation wavelength show 66 and 67%, respectively. Under standard global AM 1.5 solar conditions, the **DCSC13**-

(19) Nazeeruddin, M. K.; Humphry-Baker, R.; Liska, P.; Grätzel, M. *J. Phys. Chem. B* **2003**, *127*, 8981–8987.
(20) Nazeeruddin, M. K.; Zakeeruddin, S. M.; Lagref, J. J.; Liska, P.; Comte, P.; Barolo, C.; Viscardi, G.; Schenk, K.; Grätzel, M. *Coord. Chem. Rev.* **2004**, *248*, 1317–1328.
(21) Burnside, S. D.; Shklover, V.; Barbe, C. J.; Comte, P.; Arendse, F.; Brooks, K.; Grätzel, M. *Chem. Mater.* **1998**, *10*, 2419.
(22) Nazeeruddin, M. K.; Péchy, P.; Renouard, T.; Zakeeruddin, S. M.; Humphry-Baker, R.; Comte, P.; Liska, P.; Le, C.; Costa, E.; Shklover, V.; Spiccia, L.; Deacon, G. B.; Bignozzi, C. A.; Grätzel, M. *J. Am. Chem. Soc.* **2001**, *123*, 1613.
(23) Zhang, Z.; Evans, N.; Zakeeruddin, S. M.; Humphry-Baker, R.; Grätzel, M. *J. Phys. Chem. C* **2007**, *111*(1), 398.

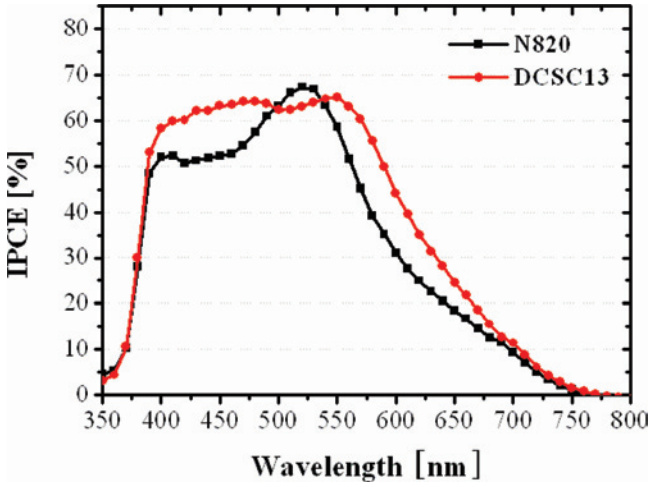

Figure 3. Comparison of incident photon-to-current conversion efficiencies plotted as a function of excitation wavelength for **DCSC13** and **N820** sensitizers anchored on nanocrystalline 2 µm thick TiO_2 films.

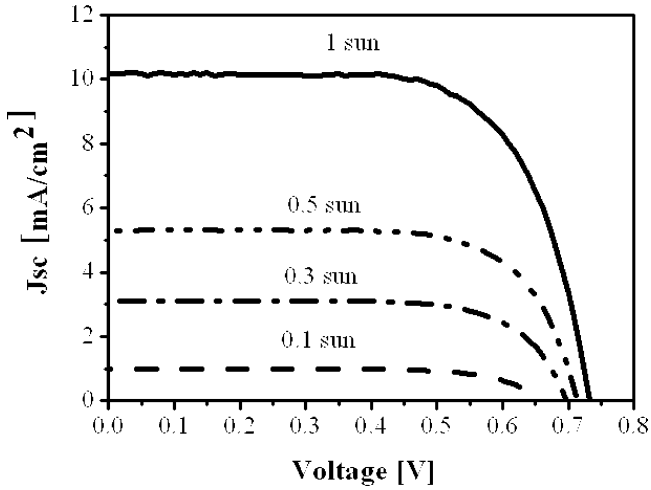

Figure 4. Photocurrent−voltage characteristics of the nanocrystalline photoelectrochemical cell sensitized with **DCSC13** under a light source that simulates global AM1.5 solar radiation 1.0 (100 mW/cm^2), 0.5 (50 mW/cm^2), 0.3 (30 mW/cm^2), and 0.1 sun (10 mW/cm^2). The cell is masked with black plastic to avoid diffusive light, leaving an active cell area of 0.158 cm^2.

sensitized cell gave a short-circuit photocurrent density (J_{SC}) of 10.1 mA/cm^2, an open-circuit voltage (V_{OC}) of 733 mV, and a fill factor (*ff*) of 0.69, corresponding to an overall conversion efficiency η, derived from the equation $\eta = J_{SC}V_{OC}ff$/light intensity, of 5.11% (Figure 4). Under similar conditions, the **N820**-sensitized cell gave a short-circuit photocurrent density (i_{SC}) of 9.00 mA/cm^2, an open-circuit voltage (V_{OC}) of 690 mV and a fill factor (*ff*) of 0.71, yielding an efficiency of 4.40%. It is striking to note that even though the adsorbed **DCSC13** sensitizer is 40% less than that of the **N820** sensitizer as a result of less adsorption of molecules onto the TiO_2 surface, the short-circuit photocurrent density is 11% higher than that of the **N820** sensitizer.

The V_{OC} of the DCSC13-sensitized cells is higher (40 mV) than the N820 sensitized cells, as shown in Figure 5. The photocurrent density varies exponentially with the photovoltage. The slopes $\partial V_{OC}/\partial \log(J_{SC})$ of N820- and DCSC13-sensitized cells were almost the same, 80 and 74 mV, respectively. The similar value of $\partial V_{OC}/\partial \log(J_{SC})$ implies

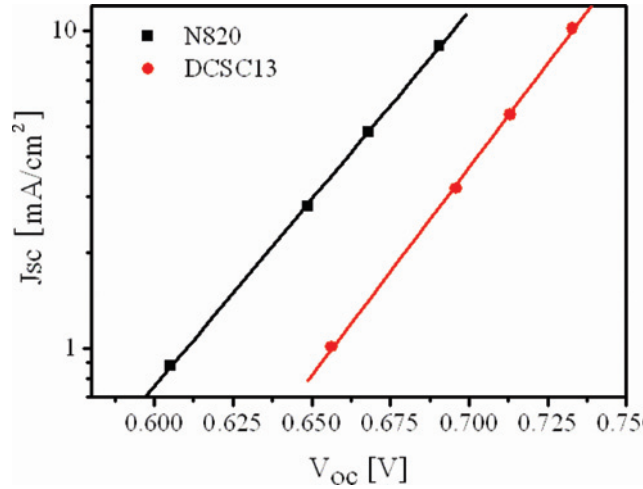

Figure 5. The short-circuit current density as a function of open-circuit voltage obtained at different light intensities from Figure 4. Transparent nanocrystalline TiO_2 film (2 µm) derivatized with a monolayer of **N820** (black) and **DCSC13** (red).

that there is no difference in transport properties of the TiO_2 nanocrystalline film in both of the cells.[21] Hence, the substituted di(2-(3,6-bis-dimethylbutoxy)ethenyl) groups in **DCSC13** do not affect the electron-transport properties in the TiO_2 nanocrystalline film. The V_{OC} of a DSSC is determined by the difference between the quasi-Fermi level in TiO_2 under illumination and the Fermi level of the electrolyte (redox potential). The increase in V_{OC} could be explained by two different mechanisms: one is the retardation of the recombination between injected electrons and oxidized species in the electrolyte, and another is the band edge movement with respect to the redox potential.[21] The electron lifetime in a DSC can be estimated from the photovoltage response to a small perturbing light pulse.[24] The apparent photovoltage decay at the open-circuit condition can be obtained from fitting to the following the exponential equation:

$$\Delta V_{photo}(t) = \Delta V_{photo}(0)\exp(-t/\tau) \qquad (1)$$

where t is the time from the end of a small light pulse and τ is the apparent electron lifetime of the electrons. The apparent electron lifetime can be obtained from fitting the photovoltage decay with an exponential function. Part (a) of Figure 6 shows a plot for the change in electron lifetime (τ) for the above-discussed dye-sensitized solar cells. At the same photovoltage, the apparent electron lifetimes (τ) in the **DCSC13**-sensitized solar cell is 2.5 times longer than that of the solar cell sensitized with the reference **N820** complex, reflecting the effect of 4,4′-di(2-(3,6-bis-dimethylbutoxy)-ethenyl) groups on the electron lifetime. The highly substituted di(2-(3,6-bis-dimethylbutoxy)ethenyl) groups prevent the triiodide in the electrolyte from recombining with injected electrons in the TiO_2 condution band, leading to increased open-circuit potentials when compared to the **N820** sensitizer. When the photoinduced charge density is plotted with the short-circuit current as shown in part (b) of Figure 6, the

(24) Duffy, N. W.; Peter, L. M.; Wijayatha, K. G. U. *Electrochem. Commun.* **2000**, *2*, 262.

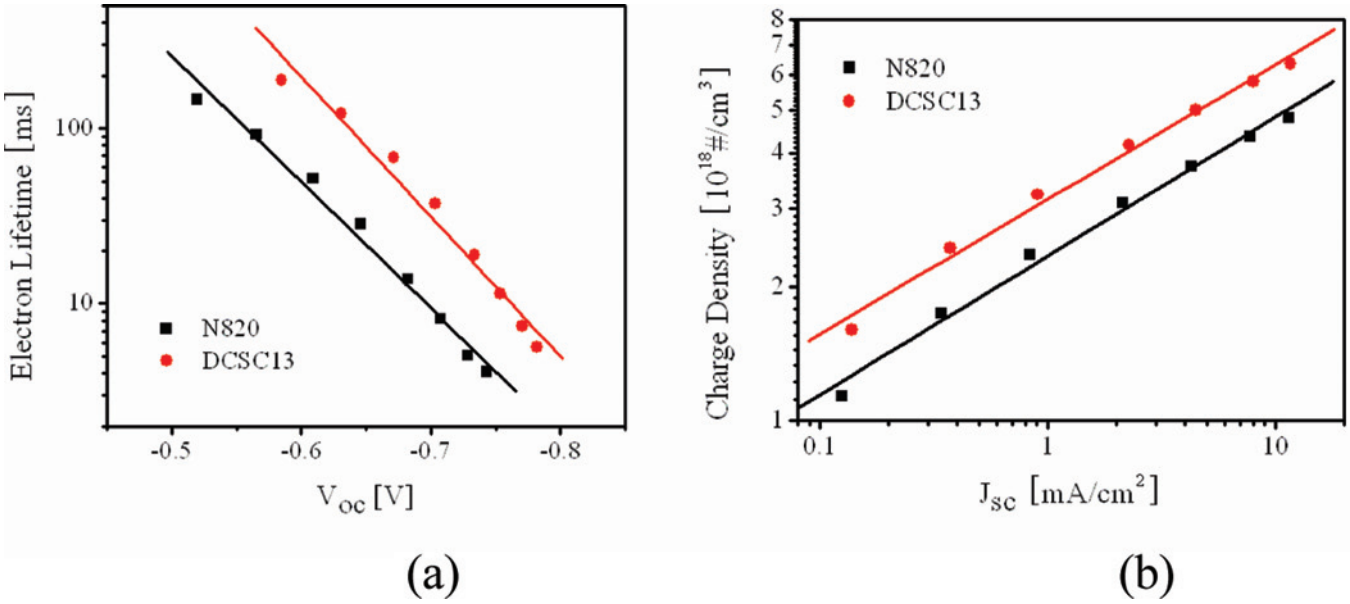

Figure 6. Electron lifetime (a) and extracted charge density (b) obtained with a 2 µm transparent nanocrystalline TiO_2 film supported onto a conducting glass sheet and derivatized with a monolayer of **N820** (black line) and **DCSC13** (red line).

recombination current is the same as the short-circuit current at open circuit for the same light intensity.[25] The measured photocurrent density (J_{SC}) is the sum of the injected current density (J_{inj}) and the recombination current density $\{J_r\}$. So, under the following conditions, at open circuit and at constant photon flux

$$J_{SC} = J_r + J_{inj} = 0, \quad J_{inj} + \{J_r\}$$

At short circuit, $J_{SC} = J_r + J_{inj} = J_{inj}$, J_r is negligible (because the transport rate is much faster than the recombination rate).[25]

Hence,

$$J_{SC} = \{J_r\} \tag{2}$$

J_{SC} is proportional to photoinduced charge density and is affected by the recombination rate and the concentration of the oxidized redox component. Consequently, a lower J_{SC} for the same photoinduced charge density implies a slower recombination process. The photoinduced charge density (n) at the open-circuit condition is given by the equation[26]

$$n = J_{SC}\tau/(q_e d(1-\rho)) \tag{3}$$

where J_{SC} is a short-circuit current density, τ is an apparent electron lifetime of electrons, q_e is the electron charge, and d is a thickness of mesoporous film having a porosity of ρ. At the same photoinduced charge density in part (b) of Figure 6, the **DCSC13**-sensitized solar cell shows a lower recombination current density, which means the substituted di(2-(3,6-bis-dimethylbutoxy)ethenyl) groups slow the recombination process (by a factor of about 2.5). To look into the effect of the band edge shift of TiO_2 on the increase in photovoltage, the photocharge density is compared with photovoltage. The higher and lower V_{OC} at the same photocharge density means a negative (upward) and positive (downward) shift of the band edge of TiO_2.[21] However, there was no critical difference of V_{OC} in the **N820**- and **DCSC13**-sensitized solar cells. Hence, the high V_{OC} in the **DCSC13**-sensitized solar cell turns out to be the result of a slower recombination process due to sterically crowded di(2-(3,6-bis-dimethylbutoxy)ethenyl) groups.

Conclusion

The noteworthy feature of this work is the development of a sensitizer with 4,4′-di(2-(3,6-bis-dimethylbutoxy)ethenyl) donor groups that provide directionality in the excited state, display enhanced oscillator strength and red-shift absorption bands. In addition, the substituted di(2-(3,6-bis-dimethylbutoxy)ethenyl) groups prevent the triiodide in the electrolyte from recombining with injected electrons in TiO_2, leading to increased open-circuit potentials. However, the disadvantage of **DCSC13** is the relatively large size of the molecule, which decreases the sensitizer uptake onto the TiO_2 surface. Thus, the **DCSC13** type of sensitizers would be more effective for the dye-sensitized solar cell with larger TiO_2 particles, and we are currently addressing research directed toward this goal in our laboratory.

Acknowledgment. This work was supported by the Korea Science and Engineering Foundation (KOSEF) through the National Research Lab. The program is funded by the Ministry of Science and Technology (Grant M10500000034-06J0000-03410) and BK 21 (2006), EU COST action D35/0007/05, and the Swiss Federal Office for Energy (OFEN). We thank Dr. K. Kalyanasunadarm, Dr. Peter Péchy, Dr. Paul Liska, and Pascal Comte for their kind assistance.

IC700996X

(25) Kopidakis, N.; Neale, N. R.; Frank, A. J. *J. Phys. Chem. B* **2006**, *110*, 12485.
(26) Kopidakis, N.; Benkstein, K. D.; van de Lagemaat, J.; Frank, A. J. *J. Phys. Chem. B* **2003**, *107*, 11307.